Research in Astron. Astrophys. **2012** Vol. **12** No. **8**, 1021–1043
http://www.raa-journal.org *http://www.iop.org/journals/raa*

Research in Astronomy and Astrophysics

The assembly of the Milky Way and its satellite galaxies *

Martin C. Smith[1,2], Sakurako Okamoto[1], Hai-Bo Yuan[1,3] and Xiao-Wei Liu[1,4]

[1] Kavli Institute for Astronomy and Astrophysics, Peking University, Beijing 100871, China; *dr.mcsmith@me.com*
[2] National Astronomical Observatories, Chinese Academy of Sciences, Beijing 100012, China
[3] LAMOST Fellow
[4] Department of Astronomy, Peking University, Beijing 100871, China

Received 2012 July 11; accepted 2012 July 17

Abstract In recent years it has become clear that the Milky Way is an important testing ground for theories of galaxy formation. Much of this growth has been driven by large surveys, both photometric and spectroscopic, which are producing vast and rich catalogs of data. Through the analysis of these data sets we can gain new and detailed insights into the physical processes which shaped the Milky Way's evolution. This review will discuss a number of these developments, first focusing on the disk of the Milky Way, and then looking at its satellite population. The importance of surveys has not gone unnoticed by the Chinese astronomy community and in the final section we discuss a number of Chinese projects that are set to play a key role in the development of this field.

Key words: Galaxy: structure — Galaxy: evolution — Galaxy: kinematics and dynamics — Galaxy: disk — galaxies: dwarf — surveys

1 INTRODUCTION

The formation and evolution of the Milky Way is a fast moving field. What was fashionable a few years ago can soon become obsolete as the focus shifts from one aspect to another. Although this rapid pace of development can make it tough to keep up with, it produces an exciting field for those involved. When compiling a review such as this, it quickly becomes apparent that even in the past months much progress has been made. As surveys blossom, producing rich and varied data sets, fresh insights and developments push the field forward into new and sometimes unexpected directions. This review will attempt to provide a brief overview of some of these recent developments, concentrating on what we can learn about the formation and evolution of the Milky Way from both the stars around us and the satellite galaxies surrounding it. This pace of development means that the review will mainly focus on a number of more recent studies, leaving eager readers to pursue the historical context at their leisure. Furthermore, we do not have space to include reviews of the Galactic bulge or halo, both of which deserve articles in their own right, restricting our dissection of the Milky Way to the properties of the disk (Sect. 2). After discussing the Milky Way's disk, we then move on to its satellite galaxies (Sect. 3). As mentioned, surveys are key to driving our understanding of the Milky Way and this fact has not gone unnoticed by the Chinese astronomy community –

* Supported by the National Natural Science Foundation of China.

therefore in the final section (Sect. 4) we will discuss a number of Chinese projects that are set to take a pivotal role in the future of this field.

2 THE ASSEMBLY OF THE MILKY WAY

We start this review with the Milky Way itself, focusing on the dominant component, at least in terms of luminosity, namely the Galactic disk. Although the vast majority of stellar mass in the Milky Way belongs to the disk ($\sim$ 90 percent), and almost all of the stars in the solar neighborhood, there are still many facets which are not well understood. We will address a number of these in this section, beginning with the global properties and then providing a more detailed look at its evolution. It is always valuable to consider the Milky Way in the context of galaxies in general and, although there is no space to do that here, one can place the Milky Way's disk in context by looking at the recent review article of van der Kruit & Freeman (2011).

Our understanding of the chemical and dynamical properties of the Milky Way disk has increased dramatically in recent years, owing to surveys such as the Geneva Copenhagen Survey (GCS; Holmberg et al. 2009), RAVE (Siebert et al. 2011a) and the Sloan Digital Sky Survey (SDSS) (Aihara et al. 2011), with its Galactic component SEGUE (Yanny et al. 2009). These span a range of volumes: GCS provides a sample of nearby F and G dwarfs out to $\sim$100 pc; RAVE is a magnitude limited spectroscopic survey ($9 < I < 13$), reaching out to around 1 kpc and 10 kpc for dwarfs and giants, respectively; SDSS/SEGUE, with optical photometry down to around 22nd magnitude and spectroscopy to 19th, can be used to probe the full vertical extent of the disk (since most of the data were taken at high Galactic latitudes, its ability to probe the disk at large radii is limited).

One of the most controversial aspects in recent years has been the nature of the thick disk. For many external galaxies it has been shown that the disk can be decomposed into two exponential components, dubbed thin and thick disks (see, for example, sect. 7 of the review by van der Kruit & Freeman 2011). A few years after the initial discovery of these thick disks, a similar claim was made for the Milky Way (Gilmore & Reid 1983), prompting numerous papers analyzing the properties and potential origins of this component. What is incontrovertible is that as one moves away from the plane of the Milky Way, the disk on average becomes hotter, more metal poor and has a larger velocity lag. What is less clear is whether this is a consequence of a mixture of two distinct components or gradients within a single entity. This question motivates much of the current analysis on disk structure and evolution, as we shall see during the course of this review.

2.1 A Broad-brush Picture of the Disk

2.1.1 Spatial distribution and chemical composition of disk stars

The above surveys have enabled researchers to obtain a more precise map of the structure of the Milky Way disk. In particular, the deep wide-field photometric survey of SDSS has provided one of the most complete pictures of the nearby disk, as presented in the thorough analysis of Jurić et al. (2008). Using distances derived from photometric relations they reproduce the findings of Gilmore & Reid, namely that the nearby density distribution is well represented by two exponential disks, with scale heights and lengths of $H_1 = 300$ pc and $L_1 = 2600$ pc, and $H_2 = 900$ pc and $L_2 = 3600$ pc, and local thick-to-thin disk density normalization of around $\rho_{\rm thick}(R_\odot)/\rho_{\rm thin}(R_\odot) = 12$ percent. Since this analysis uses SDSS, which is mostly at high Galactic latitudes ($|b| > 25$ deg), they are only able to gain a limited handle on the radial profile and hence the estimated scale-lengths are uncertain to around 20–30 percent (and unsurprisingly these two parameters are anti-correlated).

A companion paper, which followed in the same year (Ivezić et al. 2008), took this one step further, using photometric relations not only to define distances, but also metallicities. The metallicity relation was derived using spectroscopic data from SDSS and is applicable to main-sequence F- and G-type stars. Upon testing with clusters this relation was found to be accurate to within a few tenths

of a dex, extending down to a limiting metallicity of around $[\mathrm{Fe/H}] \sim -2$, below which $u-g$ is no longer sensitive to $[\mathrm{Fe/H}]$. Due to improvements in the SDSS spectroscopic metallicity pipeline, a revised relation was presented in Appendix A1 of Bond et al. (2010). The Ivezić et al. paper also presents a robust distance relation (eqs. A1–A5), which was calibrated using a set of globular clusters, then also tested using independent clusters as well as field stars. The relation is valid for dwarfs stars with $0.2 < (g-i) < 4$ and has a scatter of around 0.2 mag, although it is not clear how accurate it is for blue stars near the main-sequence turn-off (see Smith et al. 2009, 2012, for an alternative correction in this regime). These relations have proved very valuable for many researchers working with the SDSS photometric system, although such methods should be used with care, especially when analyzing kinematics (e.g. Schönrich et al. 2012).

Given these metallicity and distance relations, Ivezić et al. (2008) proceeded to investigate metallicity gradients within the disk and halo, finding the expected trend, namely that metallicity decreases smoothly with height from the plane (the median disk metallicity decreases from -0.6 at 500 pc to -0.8 beyond several kpc). The fact that the disk becomes more metal-poor away from the plane is nothing new. However, in recent years much has been done looking in more detail at the chemical properties of the disk. In the past decade many high-resolution studies have studied the disk. For example, the oft-cited work of Venn et al. (2004), who analyzed a compilation of literature sources to show that thick disk stars (or, to be more precise, disk stars which exhibit significant lag behind the local standard of rest) are more abundant in α-elements relative to iron. This is also true for disk stars which have lower $[\mathrm{Fe/H}]$ and disk stars which are at larger scale-heights, as can be seen in a number of papers (Bensby et al. 2011; Ruchti et al. 2011; Ishigaki et al. 2012). As α-elements are primarily produced in short-lived high-mass stars, this indicates that the metal-poor disk is enriched by Type II supernovae, before Type Ia supernovae have had time to provide significant iron enrichment. In other words, these stars are old and are expected to have a relatively short star formation timescale. Whether this indicates a separate component, or is just evidence for gradients within the disk population, is not clear-cut and we defer that discussion to Section 2.2. The issue of chemistry is an important one that we will refer to throughout this review, however we will not carry out a detailed review of the elemental abundances and refer interested readers to the above papers and references therein.

Returning to the issue of scale-lengths, a study similar to Ivezić et al. (2008) was carried out by de Jong et al. (2010), who used photometry to constrain the structural properties of the disk. They also found a similar thick-disk scale-length to Jurić et al. (4.1 ± 0.4 kpc), although this is arguably not surprising since the thin-disk model was fixed to that of Jurić et al.

To obtain a clearer division between these two components, it is better to use spectroscopic data. As mentioned above, SDSS also has a large number of spectra for disk stars, from the Galactic component of the survey SEGUE (Yanny et al. 2009). These data have been used in two separate studies (Bovy et al. 2012a; Cheng et al. 2012) both of which found differing results to Jurić et al., preferring a short thick disk and a long thin disk. For example, Cheng et al. (2012) claim scale-lengths of ~ 3.4 kpc and ~ 1.8 kpc for the thin and thick disks, respectively. Although these findings differ from both Jurić et al. and de Jong et al., remember that Jurić et al. found an anti-correlation between the scale-lengths of the thin/thick disks and so these results may not be in conflict. Evidence for a stubby thick disk are not restricted to SDSS/SEGUE, for example a recent independent study by Bensby et al. (2011) finds similar results.

2.1.2 Kinematic studies

Kinematics of stars can also be used to investigate the disk of the Milky Way. As has already been mentioned, the metal-poor stars in the disk lag behind the local standard of rest much more than the metal-rich stars. It is a well-known phenomenon that a population of stars with larger velocity dispersion exhibits a greater lag in rotational velocity – this is commonly referred to as the asymmetric

drift (see, for example, sect. 10.3.1 of Binney & Merrifield 1998) and is clearly evident in the solar neighborhood (e.g. Dehnen & Binney 1998a). Large surveys, both photometric (proper motions) and spectroscopic (radial velocities), are now enabling detailed kinematic analyses of the properties of the disk as one departs from the plane. A selection of studies from recent years includes the following: Spagna et al. (2010); Carollo et al. (2010); Casetti-Dinescu et al. (2011); Kordopatis et al. (2011); Bovy et al. (2012c); Sanders (2012); Cheng et al. (2012); Smith et al. (2012).

Tracing kinematic properties of the disk can be tricky and there are a number of issues which need to be carefully considered, some of which affect the above studies. One aspect is that of contamination from the halo. As one reaches the tail of the metal-poor disk, there can be non-negligible overlap between the velocities of the disk and the halo populations as the large lag and large dispersion overlaps with the halo, which has dispersion in v_ϕ of ~ 80 km s^{-1}(e.g. Smith et al. 2009). An extreme example of this can be seen in the lower-left panel of Figure 1. This becomes more of a problem as one reaches larger heights from the plane, but is even present in the solar neighborhood where the metal-poor tail of the disk and the metal-rich tail of the halo overlap around $[\mathrm{Fe/H}] \sim -1$. Another complication which is often neglected is that the velocity distribution of the disk is not well-represented by a Gaussian distribution. The aforementioned asymmetric drift induces a tail into the distribution for smaller velocities (also shown in the lower-left panel of Fig. 1). Although this is negligible for metal-rich populations close to the plane, for hotter populations the distribution can become significantly skewed. In order to overcome this, one can use more realistic functional forms, such as the distribution function of Binney (2010) or the simplified analytic formula of Schönrich & Binney (2012).

Due to gradients in these populations, it is not possible to quote single values for the kinematic properties of the disk unless one is specific about the metallicity range and at which location. An illustration of this issue is given in Figure 1, which shows how both dispersion and mean rotation velocity vary as a function of metallicity and height from the plane. As expected, more metal-poor populations are hotter, as are those further from the plane, and these trends are accompanied by a corresponding increase in velocity lag. Beyond this one can use dispersion ratios to analyze heating, for example by studying the ratio of in-plane to out-of-the-plane heating via the ratio σ_z/σ_R. The observed kinematics can then be used to constrain, or at least confront, models of Milky Way disk formation. The lower-right panel of Figure 1 shows the predictions from the model of Loebman et al. (2011), as provided by Victor Debattista (private communication), which is derived from a high resolution N-body simulation including smooth particle hydrodynamics. Note that even though this model was not fine-tuned to reproduce kinematic gradients in the disk, it is able to qualitatively match the observed properties with remarkable success. However, we leave a more detailed analysis of the kinematics of the disk, investigating orbital properties and comparisons to models, to Section 2.2.

2.1.3 Mass distribution

Before we leave our broad-brush review of the disk, there is one final topic which should not be neglected, namely how we can use kinematics to probe the mass distribution of the disk. This is a very powerful technique since kinematics can probe the total mass distribution, be that dark or luminous, unlike the above methods based on number counts. As we trace the total mass distribution out of the plane we can compare this to the (known) mass from the luminous disk and hence constrain the local dark matter density, which is a crucial piece of information for direct dark matter detection experiments (Peter 2011). Since most of the visible mass in the disk is contained below around 1 kpc (see Fig. 2), by analyzing populations at these distances from the plane it is possible to probe the dark matter distribution. The seminal work in this field is the series of papers by Kuijken & Gilmore (1989a,b,c, 1991), culminating in the determination of the surface mass density within 1.1 kpc of the plane, which they found to be $71\pm6\ M_\odot\ \mathrm{pc}^{-2}$ (Kuijken & Gilmore 1991) with a corresponding local dark matter density of around 0.01 $M_\odot\ \mathrm{pc}^{-3}$ (eq. (23) from Garbari et al. 2012). In the intervening

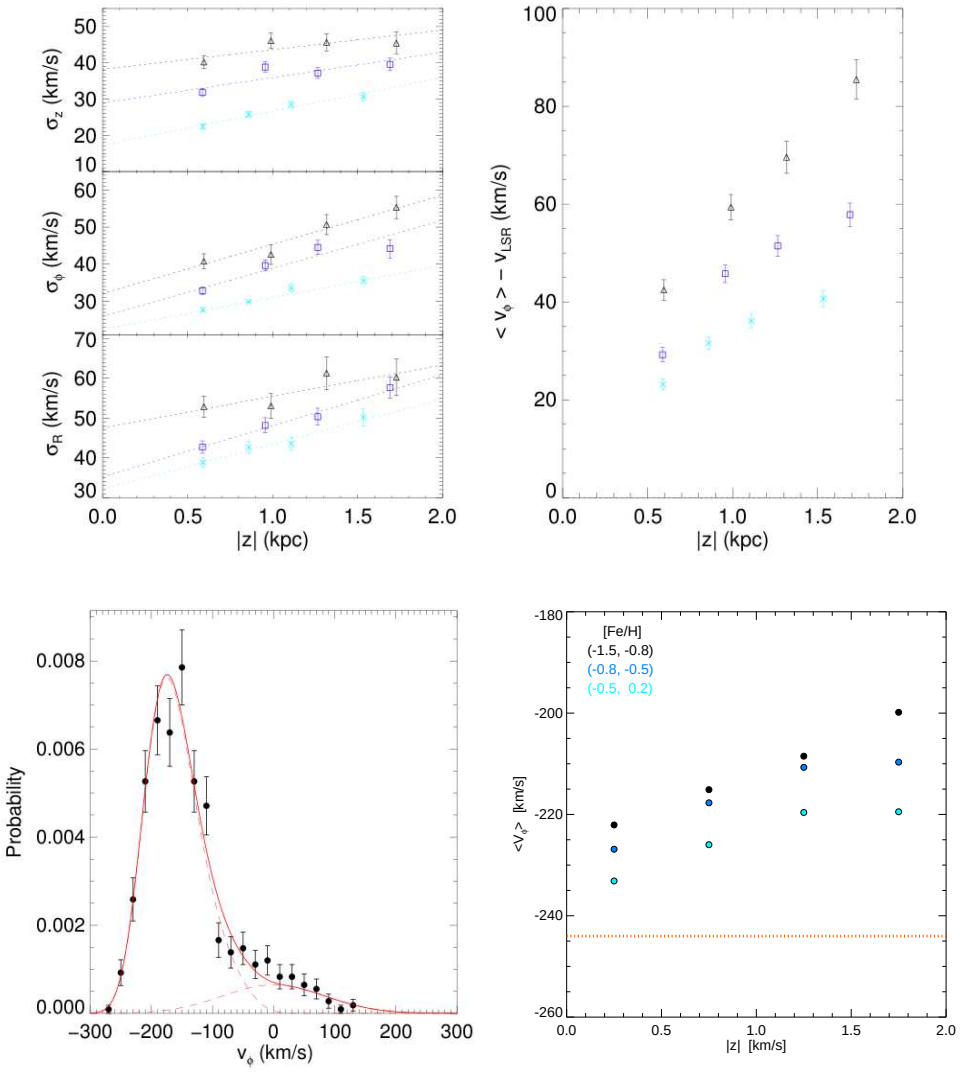

Fig. 1 A selection of results showing the kinematics of the disk from Smith et al. (2012), alongside a prediction from the model of Loebman et al. (2011, *lower-right panel*; the horizontal line denotes the circular speed of this model). The *lower-left panel* shows a fit to the rotational velocity for a sample of SDSS stars (with $[\mathrm{Fe/H}] \sim -1$ dex and $z \sim -1.7$ kpc), illustrating two of the complications that can arise, namely non-Gaussianity in the disk velocity distribution and contamination from the halo population. The *upper panels* show the resulting dispersions and mean rotation velocity once these two issues have been taken into account (see table 2 of Smith et al. 2012 for the linear fits to these dispersions). Note how the prediction from Loebman et al., although not fine-tuned to reproduce kinematic gradients in the disk, is able to qualitatively match the observed properties with remarkable success. Throughout this figure the *black*, *blue* and *cyan* points correspond to metallicity ranges $-1.5 \leq [\mathrm{Fe/H}] \leq -0.8$, $-0.8 \leq [\mathrm{Fe/H}] \leq -0.5$ and $-0.5 \leq [\mathrm{Fe/H}]$, respectively.

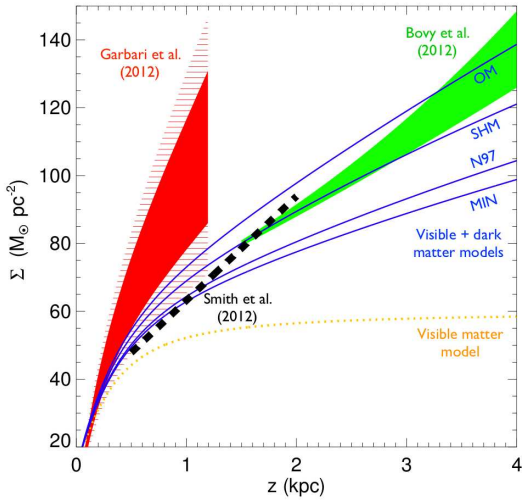

Fig. 2 Surface mass density of the disk versus height from the plane. Three observational results are included: the *red region* shows the results of Garbari et al. (2012, where the *solid region* denotes the 1-sigma confidence interval and the *hatched region* their 90-percent interval), the *thick dashed line* (Smith et al. 2012) and the *green region* (Bovy & Tremaine 2012, where this region corresponds to a thick-disk scale-length of 2 kpc and includes a correction for the dependence of circular velocity on z). These can be compared to the classical result of Kuijken & Gilmore (1991), who found a mass of $71 \pm 6\ M_\odot\ \mathrm{pc}^{-2}$ within 1.1 kpc. The *thin lines* show model predictions from the literature, with the *lower dotted curve* denoting a model including only visible matter and the *four upper solid curves* denoting models including dark matter; for example SHM corresponds to the standard halo model which has a local dark matter density of $0.01\ M_\odot\ \mathrm{pc}^{-3} = 0.38\ \mathrm{GeV\ cm}^{-3}$. This figure is adapted from Bovy & Tremaine (2012), where details of the literature models can be found.

twenty years a number of works have attempted to build on this, yet until recently this was still the standard reference (see fig. 1 of Garbari et al. 2011 for a comparison of recent measurements). However, we are now in the era of large spectroscopic surveys and as more data are amassed, more precise measurements will be possible. In the past year there has been a flurry of papers (e.g. Bovy & Tremaine 2012; Smith et al. 2012; Garbari et al. 2012) and this is likely to continue as new datasets are analyzed. These three works are summarised in Figure 2, which shows how the mass density varies with distance from the plane. The Smith et al. (2012) paper presents one of the first attempts to do this using SDSS data; although they are not able to place very robust constraints on the local density of dark matter, they do find good agreement with mass models of Dehnen & Binney (1998b), in particular matching well the least halo-dominated model where the disk (which has a relatively short scale-length) dominates the circular speed at the solar neighbourhood (see the top panel of fig. 9 in Smith et al. 2012).

2.2 A More Detailed Look at the Disk: Orbital Properties of Disk Stars, Migration and Resonances

The velocity distribution of the solar neighborhood is rich in detail, providing many clues as to the disk's formation and evolution. In this section we will look at the distribution, reviewing some of the properties and mechanisms which affect the kinematics of stars in the disk.

2.2.1 Moving groups and kinematic substructure

The analysis of solar-neighborhood kinematics has been going on for many years, but recently it has become possible to make more robust studies due to large samples of stars with accurate 3D velocity information. Significant progress in this field was afforded by the Hipparcos satellite, which measured accurate proper motions and parallaxes for tens of thousands of nearby stars. An influential couple of papers analyzing the solar-neighborhood kinematics using Hipparcos stars were published in 1998 (Dehnen & Binney 1998a; Dehnen 1998). The latter of these shows that the velocity distribution is far from the smooth profile which one would expect from well-mixed orbits in an un-evolving axisymmetric potential. However, it is not surprising that the Milky Way, with all its complexities, does not behave according to those naive approximations.

For example, the presence of a bar in the central region, transient spiral arms and dissolving star clusters can all work to cause substructure in the velocity distribution. As well as substructures, it appears that net motions may also be present (e.g. Siebert et al. 2011b; Smith et al. 2012), which are again a feature of a potential that is either evolving or deviates from axi-symmetry. However, small net motions can also be a consequence of mistaken assumptions; for example Smith et al. (2012) remark that their net radial motion could be explained by a revision of the Sun's motion with respect to the local standard of rest, which has subsequently been advocated by Schönrich (2012).

These are not new phenomena, with the first discoveries going back over a hundred years (e.g. Kapteyn 1905), but it is now possible to carry out analyses on statistically large samples and learn more about their diverse origins. Some of these groups contain stars of a similar age and metallicity, often young stars, implying they are simply star clusters in the process of disrupting. Other features in this diagram contain stars with a range of ages and hence cannot be due to young dissolving clusters; these features are more likely caused by resonances due to features in the potential (e.g. the bar or spiral arms). A discussion of these features is presented in Famaey et al. (2005), although this is only one of many such papers. A more recent study was carried out by Antoja et al. (2012), who used data from the RAVE survey to show that many of these features have a significant spatial extent, reaching as much as $\sim$1 kpc within the plane and also $\sim$700 pc out of the plane. Another study tracing velocity structure outside the solar neighborhood has been presented in Liu et al. (2012), who identified a notable bifurcation in the radial component of the velocity in observations towards the anti-center (see Fig. 3). As well as substructures, it appears that net motions are also present (e.g. Siebert et al. 2011b; Smith et al. 2012), which are again a feature of a potential that is either evolving or deviates from axi-symmetry.

Attempts to identify origins for specific features have been carried out by numerous authors. For example, the Hercules stream, which consists of a group of stars moving radially outward and lagging behind the local standard of rest, is commonly thought to originate from stars in resonance with the Galactic bar (e.g. Dehnen 2000; Fux 2001). Such features are important as they can be used to constrain the properties of the bar, such as the pattern speed, particularly if we can trace such features across multiple locations in the disk (e.g. Bovy 2010). The situation becomes more complex when one considers resonances due to spiral arms (e.g. De Simone et al. 2004; Quillen & Minchev 2005) and their overlap with bar resonances (e.g. Minchev & Famaey 2010; Quillen et al. 2011).

However, even that is not the end of the story as there are also mergers with satellite galaxies, which can leave behind streams in the local velocity distribution (e.g. Helmi et al. 2006a) or excite density waves with relatively long-lived signatures in velocity space (so-called "ringing" Minchev et al. 2009; Gómez et al. 2012a,b; Widrow et al. 2012). In order to disentangle all of these features requires data of exquisite precision. Fortunately we may not have to wait too long for this to happen, as the upcoming Gaia satellite mission will measure accurate proper motions and parallaxes to millions of stars in the solar neighborhood.

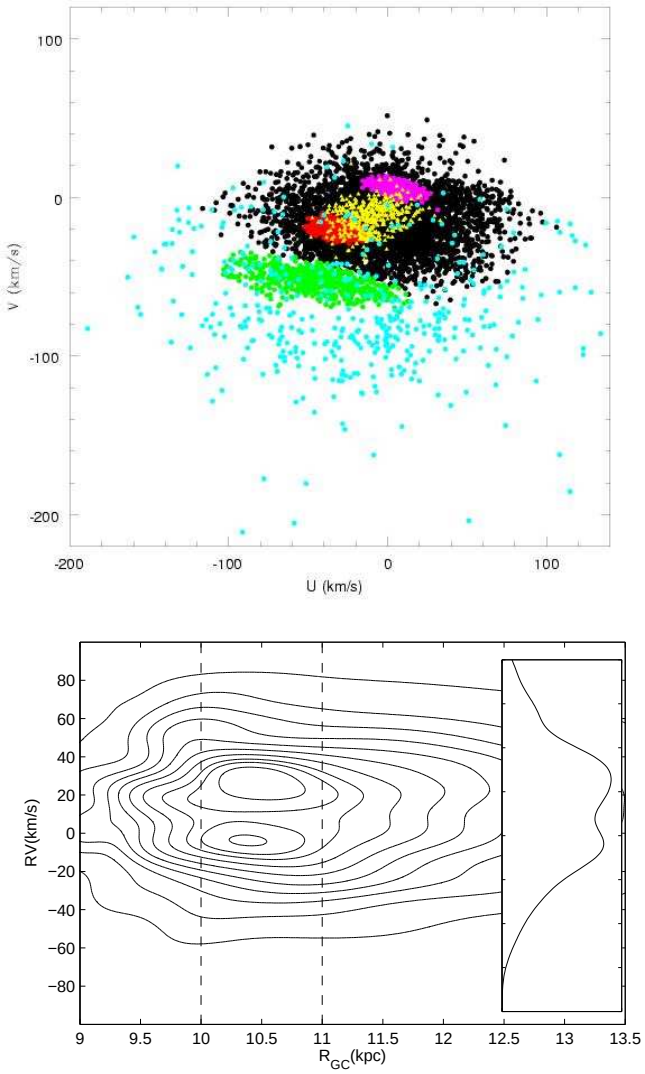

Fig. 3 Examples of kinematic substructure in the disk. The *top* panel shows the velocity distribution for nearby K- and M-giants (Famaey et al. 2005), illustrating a number of the different moving groups (for example, the Hercules group is denoted by the *green points*). The *bottom* panel presents an example of kinematic substructure outside the solar neighborhood, showing how the radial velocity of stars toward the anti-center (i.e. equivalent to $-U$ in the top panel) varies with Galacto-centric distance (Liu et al. 2012). A clear bifurcation in velocities is present between 10 to 11 kpc, as highlighted by the inset which shows the velocity distribution for all stars in this 1 kpc slice.

2.2.2 Mechanisms to create kinematic substructure in the disk

With all of these processes ongoing in the disk, a star will find it hard to enjoy a quiet life. Although commonly assumed to be born on approximately circular orbits, as stars are buffeted by these various mechanisms, they can be scattered away from their original orbits and birth radii. These processes,

along with other mechanisms such as interactions with giant molecular clouds, work to heat the disk, leading to correlations between velocity dispersion and age (e.g. fig. 7 of Holmberg et al. 2009; see also Seabroke & Gilmore 2007). This scattering of stars away from their birth radii leads to migration within the disk. The topic of migration has become crucial to our understanding of disk evolution. The seminal paper in this field is that of Sellwood & Binney (2002), with a number of later contributions (including Roškar et al. 2008; Schönrich & Binney 2009a,b; Minchev & Famaey 2010). This pair of Schönrich & Binney papers is particularly useful in elucidating the effects of migration, by incorporating radial mixing into a chemical evolution model. This radial mixing is classified into two schemes. The first of these, dubbed blurring, refers to the gradual heating of stars over time, as processes work to increase orbital eccentricity and lead to stars oscillating around their guiding centers. The second scheme, churning, is an implementation of the mechanism described in Sellwood & Binney (2002). This describes how stars change angular momenta over time, which occurs when a star is at the corotation resonance with a spiral arm. This shifts the guiding centers of their orbits, but does not alter their eccentricities (and hence does not work to heat the disk). One outcome of this is that it substantially increases the chemical heterogeneity of the stars that one finds near the Sun with a given rotation velocity, as stars from different birth radii migrate to the solar neighborhood by changing their angular momentum. Although this Schönrich & Binney model is constructed with simplified prescriptions, its value lies in how it gives the reader a clear picture of the underlying processes and, at the same time, is able to provide a very good match to observational data.

2.2.3 Dissecting the disk using α-element abundances

Given these processes which lead to disk heating and migration, the question that naturally arises is whether they are able to create the thick disk that we see today. Although this is an easy question to pose, it is a very difficult and controversial one to answer.

As mentioned previously, α-element abundances are very important for dissecting the components of the disk because $[\alpha/\mathrm{Fe}]$ can be used as a proxy for age. The daunting task of estimating α-element abundances from the low-resolution ($R \sim 1800$) SDSS spectra has been carried out by Lee et al. (2011a). Although obtaining α-elements from such low-resolution data can have traditional abundance experts up in arms, for statistical analyses the results should be perfectly acceptable provided the samples are treated carefully, i.e. even though the $[\alpha/\mathrm{Fe}]$ ratio for an individual star may be subject to large uncertainties, it is possible to average over a population of stars to determine trends in the data. A similar study by Boeche et al. (2011), which is also unlikely to please the traditionalists, has shown how α-element abundances can be measured for RAVE data. The problem here is that even though the RAVE resolution is higher than SDSS ($R \sim 7\,500$), these spectra have limited wavelength coverage spanning only the Ca-triplet region at 8410–8795 Å. Both of these papers include laborious verification work, comparing their results to observations taken at higher resolution, assessing stability across repeat observations, and (in the case of Lee et al. 2011a) verifying that the measured $[\alpha/\mathrm{Fe}]$ is in agreement with literature values for the open and globular clusters contained in the SDSS catalog. The conclusion of both of these studies is that provided the signal-to-noise is sufficient (typically above 30 or so), then it is possible to measure $[\alpha/\mathrm{Fe}]$ to around one or two tenths of a dex. The drawbacks compared to detailed abundances from high resolution spectra are clear, but these negatives are offset by the huge volumes of data that are now available from such low-resolution studies, currently numbering in the hundreds of thousands of stars from SDSS and RAVE alone.

Once these α elements are in hand, one can begin slicing the disk. The inaugural SDSS paper to tackle this challenge was Lee et al. (2011b). They found a bimodal distribution of $[\alpha/\mathrm{Fe}]$ (see Fig. 3 for a similar plot) and used this to define two disk components – an old hot disk with high $[\alpha/\mathrm{Fe}]$ and a younger cold disk with low $[\alpha/\mathrm{Fe}]$. One of their most interesting results came from

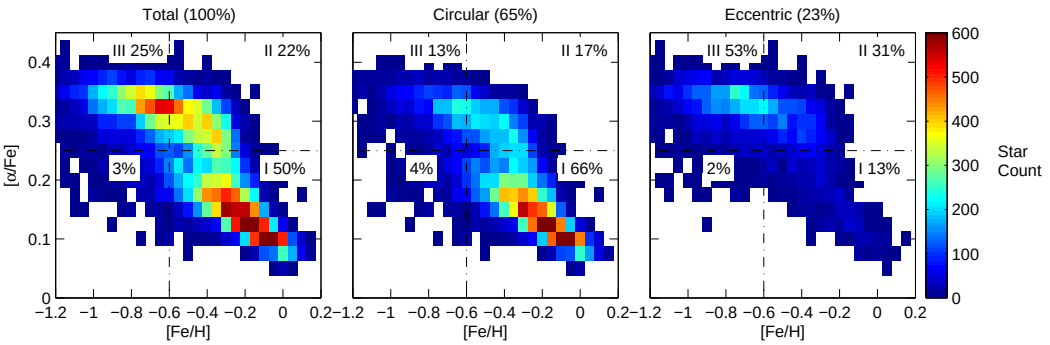

Fig. 4 The orbital properties of SDSS G dwarfs from Liu & van de Ven (2012), using data from Lee et al. (2011a). This shows the number density of G dwarfs, after correcting for the selection function. Of particular interest are the alpha-rich (i.e. likely old) stars on near-circular orbits, since these are likely a product of radial migration within the disk.

the analysis of the rotation velocity. For the old stars, they found the same trend as discussed above, namely that the more metal poor stars exhibit a larger lag. However, for the young stars they found the opposite trend, with the metal-poor stars actually exhibiting faster rotation than the metal-rich ones. The gradients vary with height from the plane, from $+40$ to $+50$ km s^{-1} dex^{-1} for the old population and from -20 to -30 km s^{-1} dex^{-1} for the young population. This is not the first study to find this trend for the young stars (see fig. 11 of Loebman et al. 2011 who observed the same trend from the Geneva-Copenhagen survey), but the quality of the SDSS data allows for this precise measurement.

Such behavior has been predicted from models and is a consequence of the above processes which stir up the disk. The reason for this correlation is that the aforementioned blurring, which gradually increases the stars orbital eccentricity over time, leading to stars in the solar neighborhood having a range of guiding center radii; some solar neighborhood stars have guiding centers further out in the disk and are therefore near the peri-centers of their orbits, whereas some have guiding centers closer in and are therefore near the apo-centers of their orbits. Due to the conservation of angular momentum on an orbit, those stars near their pericenters will have a larger rotation velocity than those near their apocenters. Then, since there is a radial metallicity gradient in the disk, with the outer parts of the disk being more metal poor (e.g. Balser et al. 2011), this means that on average those faster rotating stars with larger guiding center radii will have a lower metallicity and vice versa. This behavior has been predicted also by models, for example Schönrich & Binney (2009a, fig. 4) and Loebman et al. (2011, fig. 10). There is also an indication that the correlation between [Fe/H] and rotation velocity becomes weaker with age both in the data (fig. 11 of Loebman et al. 2011 for an analysis of GCS data; see also Yu et al. 2012 for an analysis including RAVE data) and the simulations (fig. 10 of Loebman et al. 2011), which some authors argue is a consequence of migration within the disk (churning) working to erase the metallicity gradient for the older stars.

2.2.4 Does the Milky Way have a distinct thick disk?

Although interesting, this trend does not directly address the issue of the existence, or formation, of the thick disk. A second analysis of the SDSS data, by Liu & van de Ven (2012), helps to shed light on the situation. Building on the work of Lee et al. (2011b), they looked at the distribution of orbital eccentricities for stars in the [Fe/H]–[α/Fe] plane. Although previous studies have looked at orbital eccentricities (e.g. Sales et al. 2009; Dierickx et al. 2010; Wilson et al. 2011), the availability

of $[\alpha/\mathrm{Fe}]$ allows them to gain a deeper understanding of the formation history of the disk. The work of Liu & van de Ven is summarized in Figure 4, which shows the distribution of stars in this $[\mathrm{Fe/H}]$–$[\alpha/\mathrm{Fe}]$ plane for stars on near-circular and eccentric orbits, where they use the relative-to-circular angular momentum L_z/L_c as a dynamical measure of orbital circularity, as this is less sensitive to the adopted underlying mass model for the Milky Way (see the bottom middle panel of their fig. 8). After correcting for the selection function, which in effect gives them a volume limited sample in the approximate distance range 0.5 to 4 kpc, they obtain the distribution shown in Figure 4.

From this analysis they find that the majority of stars on circular orbits are, as expected, young (with low $[\alpha/\mathrm{Fe}]$) and metal rich. However, of interest are the older stars (with high $[\alpha/\mathrm{Fe}]$) on circular orbits, which account for around a third of this sample. Liu & van de Ven argue that these stars have most likely undergone radial migration and remark that a number of properties match those predicted by the simulations of radial migration (in particular Loebman et al. 2011), such as a weakening of the rotation-metallicity anti-correlation with age. However, since radial migration tends to transfer stars from one circular orbit to another, this cannot explain the presence of old stars in the plot of stars on eccentric orbits (right panel of Fig. 4). These stars are almost exclusively old stars (with high $[\alpha/\mathrm{Fe}]$), with large velocity dispersion and scale-height, and the interpretation preferred by Liu & van de Ven is that these are a product of an early gas-rich merger (e.g. Brook et al. 2004) leading to in-situ formation of this population. However, there are multiple possible explanations (such as accretion or heating through mergers or the secular phenomena discussed above) and the truth may well be a combination of these. It should be noted that in their analysis, stars which would normally be associated with the thick disk (i.e. those at large distances from the plane) contain both near-circular and eccentric orbits, which is even more evidence that there are likely multiple mechanisms at play in creating this vertically extended component. Is this paper able to conclusively say whether there is a clear two-component thin and thick disk? Although Liu & van de Ven appear to be advocating that there is a separate thick disk formed via an early gas-rich merger, this result is not decisive.

This leads us to our final series of papers on this subject, namely the work of Bovy et al. (2012a,b,c). These papers analyzed the same SDSS data from Lee et al. (2011a), but came to somewhat different conclusions than the above authors. This series is notable for the provocatively titled paper "The Milky Way Has No Distinct Thick Disk" (Bovy et al. 2012b). Whether or not that bold claim is true, one should not overlook the primary result from the preceding paper (Bovy et al. 2012a); they find that when they divide the $[\alpha/\mathrm{Fe}]$–$[\mathrm{Fe/H}]$ plane into small "mono-abundance" bins, both the vertical and radial distribution of stars within each bin is well fit by a single exponential distribution, with a scale-height/length that varies with position in this 2D abundance plane (and, intriguingly, these populations also appear to be nearly isothermal; Bovy et al. 2012c). This surprising finding was followed up in the 2012b paper, where they apply a correction to account for the biases induced in the spatial and mass sampling from the selection function. Both of these biases act to make metal-poor and α-enhanced subpopulations more prominent in the Lee et al. (2011b) sample, owing to the fact that these SDSS data lie at high-latitudes and are color-selected. One outcome of this bias is that it can enhance the bimodality in the $[\alpha/\mathrm{Fe}]$–$[\mathrm{Fe/H}]$ plane, i.e. Bovy et al. argue that the strong bimodality, which Lee et al. (2011b) observe, is a consequence of the selection function and the bias-corrected version is fully consistent with chemical evolution models which have a smooth age distribution (e.g. Schönrich & Binney 2009a). However, their strongest argument against a thin/thick-disk decomposition is presented in fig. 2 of Bovy et al. (2012b). They estimate the surface mass density in each of their mono-abundance bins and then calculate how the total surface mass density varies as a function of scale-height. Upon finding that this is a monotonically decreasing function, with no hint of bimodality, they conclude that there cannot be a distinct thick disk. Detractors of this work will argue that there is still scope for hiding a second component within this figure and that the quality of the SDSS data is insufficient to make such a bold claim, but it has certainly fueled the debate. Perhaps the arrival of large datasets with detailed abundances, such as

those from the ongoing Gaia-ESO VLT survey (Pancino & Gaia-ESO Survey consortium 2012) or the upcoming HERMES project (Barden et al. 2010), will conclude this debate, but in the coming years this is likely to remain a contentious topic and will stay at the forefront of the field.

3 DWARF SATELLITES OF THE MILKY WAY

Dwarf galaxies are the simplest and most numerous galaxies in the Universe and their study provides clues about the formation and evolution of galaxies in a range of environments. Around the Milky Way, there are many dwarf galaxies gravitationally bound to our Galaxy. Most of the satellites are so-called dwarf spheroidal (dSph) galaxies having absolute magnitudes fainter than $\mathrm{M_B} = -14$, approximately spheroidal shape, and are only discovered, so far, in the Local Group (Mateo 1998; van den Bergh 1999). The photometric and spectroscopic studies of dSphs show that they have little or no gas and no recent star formation (e.g. Smecker-Hane et al. 1994; Tolstoy et al. 2003; Venn et al. 2004). Until 2005, only nine "classical" dSphs (Sagittarius, Fornax, Leo I, Scupltor, Leo II, Carina, Sextans, Draco, and Ursa Minor) and two irregular galaxies (Large Magellanic Cloud and Small Magellanic Cloud) were known. Thanks to wide-field photometric surveys, such as SDSS (e.g., York et al. 2000), a dozen new farther faint satellites (ultra faint dwarf galaxies, UFDs) and sub-structures were discovered in the Galactic halo (e.g. Willman et al. 2005; Belokurov et al. 2007).

3.1 Stellar Populations

The proximity of Galactic dSphs offers a unique opportunity for investigating galaxy formation and evolution in unprecedented detail by studying photometric properties of the resolved stellar populations. The population's complexities are found in bright dSphs, such as Fornax and Leo I, which contain young stars ($<$ a few Gyr) as well as old (> 10 Gyr) ones (e.g., Monelli et al. 2003; Battaglia et al. 2006; Tolstoy et al. 2009). Only the brightest two dSphs, Sagittarius and Fornax, have a few globular clusters with different metallicities (Letarte et al. 2006; Giuffrida et al. 2010), which are also the sign of multiple stellar populations. The most remarkable case is Carina dSph, which shows three completely distinct main-sequence turn offs in deep color-magnitude diagrams (e.g., Hurley-Keller et al. 1998; Monelli et al. 2003). It consists of three separate episodes of star formation, with the SFR apparently going to zero in the intervening time. The fainter dSphs, such as Ursa Minor, essentially show a single old population (e.g., Carrera et al. 2002). In the case of UFDs, deep photometries confirmed that all galaxies, except for CVn I dSph and Leo T dwarf, are all old (Coleman et al. 2007; Okamoto et al. 2008, 2012; Brown et al. 2012).

3.2 Metal Abundances

The Galactic dSphs are probably the survivors of the merging and agglomeration processes of the Milky Way, as suggested in numerical simulations and semi-analytic models (e.g. Bullock & Johnston 2005). The chemical abundances of individual stars in the present-day dSphs, however, do not match those of the Galactic halo stars. Shetrone et al. (2001) first found systematically lower [α/Fe] ratios for red giant branch (RGB) stars in Draco, Sextans, and Ursa Minor dSphs compared with Galactic halo stars of similar metallicity. The same trends were also found in the other dSphs (e.g. Shetrone et al. 2003; Sadakane et al. 2004; Aoki et al. 2009).

Figure 5, taken from Tolstoy et al. (2009), shows [α/Fe] ratios for two α-elements (Mg, Ca) of stars in Fornax, Sculptor, Sagittarius, and Carina dSphs along with a sample of Galactic halo and disk stars. The dSph stars are well separated from the majority of Galactic stars, and stars in each dSph also show different abundance patterns. However, recent spectroscopic studies revealed that the abundance patterns in the extremely metal-poor stars ([Fe/H] < -2.5) in dSphs are similar to those of low-metallicity halo stars (Frebel et al. 2010a; Tafelmeyer et al. 2010). Although the number of

observed stars is still small, this similarity implies that these metal-poor stars in dSphs were formed at the site that is similar to where the Galactic halo stars were born.

The [α/Fe] ratios make it possible to estimate how Type Ia supernovae (SNe Ia) contributed to the chemical enrichment during the early stage of galaxy formation. The α-elements, such as Mg, Si, Ca, and Ti, are produced primarily in high-mass stars and are ejected by Type II supernovae (SNe II), but Fe is produced in both SNe Ia and SNe II. The lifetime of an SNe Ia progenitor is longer than that of SNe II, so that the stars, which formed shortly after the interstellar medium (ISM) had been enriched by SNe II, should have enriched [α/Fe] ratios, but stars that formed sometime after the SNe Ia contribution should have lower [α/Fe] ratios. Therefore, a galaxy which had maintained the metal enriched gas until the start of SNe Ia contribution reached a higher metallicity than a galaxy which had lost its metals *via* galactic winds or just had a low star formation rate. This difference results in a "knee" in a plot of [α/Fe] versus [Fe/H], as shown in Figure 5. The timescale for changes in the [α/Fe] ratio depends not only on the star formation history (SFH) of a galaxy, but also on the initial mass function (IMF), the SNe Ia timescale, and the timescales for mixing SNe Ia and SNe II ejecta back into the interstellar medium (e.g. Tinsley 1979; Matteucci & Recchi 2001). The variation of [α/Fe] patterns reflects the differences of the star formation and/or chemical enrichment in dSphs and the Galactic halo.

Helmi et al. (2006b) pointed out that a lack of metal-deficient ([Fe/H]< -3.0) stars was common in four Galactic dSphs (Sextans, Sculptor, Fornax, and Carina) and concluded that the progenitors of the present-day dSphs appear to have been fundamentally different from the building blocks of the Milky Way. The stellar metallicity distribution functions of dSphs, including newly discovered

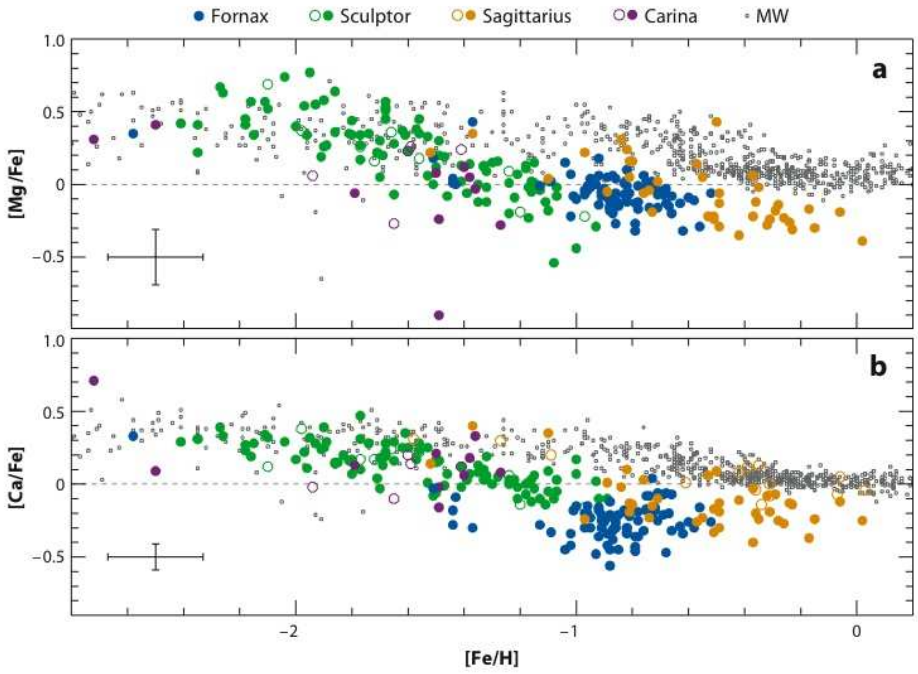

Fig. 5 [Mg/Fe] and [Ca/Fe] ratio against [Fe/H] metallicity. The *blue*, *green*, *orange* and *purple circles* represent Fornax, Sculptor, Sagittarius, and Carina dSphs, respectively, with the Galactic stars shown in *grey dots* (Tolstoy et al. 2009).

fainter ones, were updated by Kirby et al. (2008, 2011), which revealed that the metallicities of fainter satellites are lower than those of luminous dSphs, and the stellar metallicity distribution functions are similar to the metal-poor end of the Galactic halo. These results imply that the Galactic halo could have been built from less luminous satellites similar to these UFDs.

3.3 Missing Satellite Problem

One of the most famous and serious mysteries of formation of the Milky Way is the "missing satellite problem." The cold dark matter (CDM) scenario predicts a few hundred sub-halos within a Milky Way size galaxy, but only dozens of Galactic satellites are actually known. This was first noted by Moore et al. (1999) and Klypin et al. (1999), who showed cosmological models reproduced well the number of actual substructures on galaxy cluster scales, but overestimated the number on Galactic scales. Some authors subsequently suggested that in low-mass halos, gas accretion and star formation have been suppressed by photoionization due to the UV background, so that only halos formed before re-ionization of the Universe could form stars (e.g., Gnedin 2000; Somerville 2002; Susa & Umemura 2004). Other effects, such as the SNe feedback and the tidal effect, could also suppress star formation in low-mass halos (e.g., Larson 1974; Efstathiou 2000). If star formation was suppressed, the low-mass halos would become invisible satellites. Another proposed solution is the modification of properties of dark matter that eliminates the low-mass halos themselves (e.g., Zentner & Bullock 2003). If we consider warm dark matter (WDM) instead of CDM, the lowest halo-mass limit of collapse becomes higher, because WDM particles have free-streaming length longer than the CDM particles. This leads to the formation of fewer low-mass halos.

From an observational point of view, there could also be incompleteness of detection. In recent years, very faint Galactic satellites were discovered in deep photometric surveys. However, the detection of low surface brightness galaxies is still limited, even in the SDSS data. The observed luminosity function starts to decrease at a magnitude fainter than $M_V \sim -5$, which is probably due to the limiting magnitude of the current surveys. Deeper photometric surveys with larger telescopes, such as LSST and Subaru/Hyper Suprime-Cam, are required to reveal a complete sample of Galactic satellites.

3.4 Ultra Faint Dwarf Galaxy

Recently, dozens of new Galactic dSphs and one isolated galaxy have been discovered in the SDSS data: Ursa Major I (UMa I; Willman et al. 2005), Canes Venatici I (CVn I; Zucker et al. 2006a), Boötes I (Boö I; Belokurov et al. 2006), Ursa Major II (UMa II; Zucker et al. 2006b), Coma Berenices (ComBer) / Canes Venatici II (CVn II) / Hercules (Her) / Leo IV (Belokurov et al. 2007), Leo V (Belokurov et al. 2008), Boötes II (Boö II; Walsh et al. 2008), and Leo T (Irwin et al. 2007). These systems are roughly 10 to 100 times fainter than the classical dSphs and even fainter than the single star Rigel ($M_V = -7.2$); they have amorphous morphology and too-low surface brightness to be found by photographic plates. Deep wide-field photometric studies have shown that fainter UFDs lie at a distance of 60–160 kpc, have a single very old ($\sim$13.5 Gyr) and metal-poor population, and have an elongated shape. On the other hand, the brightest UFD, CVn I dSph, has a relatively young population ($\sim$12.6 Gyr) and the distribution of horizontal branch stars suggests that the galaxy contains complex stellar populations (Coleman et al. 2007; Okamoto et al. 2008, 2012). Ultra-deep HST/ACS photometry also confirms that three faint UFDs have no evidence for intermediate-age populations, and the ages are synchronized to within $\sim$1 Gyr of each other (Brown et al. 2012).

Medium-resolution spectroscopic observations have recently revealed that these UFDs have metallicities lower than luminous dSphs, and the stellar MDF is similar to the metal-poor tail of the Galactic halo MDF (Kirby et al. 2008). The luminosity-metallicity relation in Galactic satellites is well defined for nearly 4 dex in luminosity, and the distribution function of the metal-poor end of

the Galactic halo is well reproduced by the MDF of the UFDs. This implies that the low metallicity part of the Galactic halo could have been built from less-luminous satellites similar to these dim dSphs. If the UFDs are indeed building blocks of the halo, we should see an abundance pattern of heavy elements that is identical to that of Galactic halo stars, giving direct evidence to support UFDs as genuine building blocks of the Milky Way. Recent high-resolution spectroscopic observations also show that eight stars in three UFDs (UMa II, ComBer, Her) have similar abundance patterns to that of Galactic halo stars of equivalent metallicity (Koch et al. 2008; Frebel et al. 2010b). The [Mg/Fe] ratios of stars in UFDs agree with metal-poor halo stars, in contrast to those of more luminous dSphs. This result implies that stars in the UFDs were formed at sites which are similar to that of the Galactic halo stars. However, the sample is clearly too small to currently derive any definitive conclusions.

4 CHINESE SURVEYS ON GALACTIC STUDIES

4.1 The LAMOST Experiment for Galactic Understanding and Exploration (LEGUE)

4.1.1 Overview

Our Milky Way plays a unique role in understanding galaxy formation and evolution. It is the only giant galaxy that can be fully resolved and studied multi-dimensionally (in 6D phase space + chemical composition). However, it is very challenging to carry out such studies for three main reasons. Firstly, there are billions of stars distributed over the whole sky. Secondly, stars suffer from serious dust obscuration in the Galactic plane. Thirdly, it is very difficult to obtain reliable distances to individual stars. However, the Guo Shou Jing Telescope (formerly called the Large Sky Area Multi-Object Fiber Spectroscopic Telescope LAMOST; Wang et al. 1996; Su et al. 1998; Xing et al. 1998; Zhao 2000; Cui et al. 2004; Zhu et al. 2006; Cui et al. 2010; c.f. *http://www.lamost.org/website/en/*) and Gaia together provide a great opportunity in advancing studies of the Milky Way in the coming years.

The Guo Shou Jing Telescope is an innovative quasi-meridian reflecting Schmidt Telescope equipped with 16 low resolution spectrographs, 32 CCDs and 4 000 optical fibers, capable of recording spectra of up to 4 000 objects simultaneously in a field of view of 5° in diameter. With an effective aperture of 3.6–4.9 m in diameter depending on telescope pointing, it can observe objects as faint as $r = 19.0$ in 1.5 hours at resolution $R = 1\,800$, under good observing conditions. The Guo Shou Jing Telescope is located in the Xinglong Station and operated by National Astronomical Observatories of China (NAOC). Following a two-year commissioning initiated in September, 2009 and a one-year pilot survey initiated in October, 2011, the Guo Shou Jing Telescope Spectral Surveys (Zhao et al. 2012), composed of the LAMOST ExtraGAlactic Survey (LEGAS) and the LAMOST Experiment for Galactic Understanding and Exploration (LEGUE), are planed to commence in the fall of 2012.

LEGUE is composed of three subsets: a spheroid survey, an anti-center survey and a disk survey, each focusing on a distinct sky area of the Galaxy and having different target selection algorithms. The spheroid survey plans to observe at least 2.5 million stars in the high Galactic latitude regions ($|b| \geq 20°$), selected from the SDSS photometry using a preferential target selection algorithm. The anti-center survey aims to obtain spectra of a statistically complete sample of about 4 million stars down to a limiting magnitude $r = 18.5$, distributed in a contiguous area of 3438 deg^2 ($-30° \leq b \leq +30°, 150° \leq l \leq 210°$) and sampling a significant volume of the Galactic thin/thick disks and halo. The disk survey intends to cover as much area of the low Galactic latitude sky ($-20° \leq b \leq +20°$) as is visible from the Xinglong Station and can be allowed by available observing time, focusing on open clusters and selected star-forming regions in the Galactic disk.

The primary goals of LEGUE include (Deng et al. 2012):

– Search for extremely metal poor stars in the Galactic spheroid;

– Kinematic features and chemical abundances of the thin/thick disk stars, with the goals of deriving the mass distribution (including the dark matter), the dynamical and chemical evolution, the structure and the origin of the Galactic disks;
– A thorough analysis of the disk/spheroid interface near the Galactic anti-center, with the goal of determining whether previously identified anti-center structures are tidal debris, or whether they are part disk structures;
– Discovery of stellar moving groups that may be associated with dwarf galaxies, and follow-up observations of known streams and substructures in the Galactic spheroid;
– Survey of the properties of Galactic open clusters, including the structure, dynamics and evolution of the disk as probed by open clusters;
– Search for hyper-velocity stars and determination of their creation mechanisms;
– Survey the OB stars in the Galaxy, tracing the 3D extinction in the Galactic plane;
– A complete census of young stellar objects across the Galactic plane, which provides important clues to star formation at the Galactic scale and the history of Galactic star formation.

4.1.2 The spheroid survey

The spheroid survey will obtain spectra of at least 2.5 million stars with $|b| \geq 20^\circ$ selected from the SDSS photometry, at a density of 320 stars per deg^2 or higher, in two contiguous areas in the north and south Galactic caps, respectively, totaling 5 000 deg^2 or more (Deng et al. 2012). Even with LAMOST, one cannot observe all possible targets. Unlike SEGUE in which a variety of categories of stars are targeted, with each category of stars selected with an optimized set of criteria to meet the scientific goal, the LAMOST spheroid survey aims to include stars of all possible spectral types and luminosity classes. To achieve this goal, possible targets are firstly assigned with different weights according to their r magnitudes and $(g - r)$ and $(r - i)$ colors. The targets are then randomly selected following a set of uniform survey criteria that can include essentially all blue O, B, A and white dwarf stars, and a statistically significant fraction of high-latitude F turnoff stars, K giants, M giants and stars with $0.1 < (g - r) < 1.0$ (Carlin et al. 2012). A similar target selection algorithm was adopted for the spheroid part of the LAMOST pilot survey (Zhang et al. 2012; Yang et al. 2012).

4.1.3 The disk survey

The disk survey will observe at least 3 million stars as faint as $r = 16$ at low Galactic latitudes ($|b| \leq 20^\circ$) targeting approximately 1 000 objects per deg^2, and will sample about 300 open clusters (Chen et al. 2012). Its survey area between $150^\circ \leq l \leq 210^\circ$ overlaps with the Galactic anti-center survey, with the latter selecting sources from a recently finished Xuyi photometric survey using an algorithm specifically designed for the anti-center survey (see more details in Sect. 4.2). For areas where Xuyi photometry is not available, targets of the disk survey will be selected from the UCAC3 (Zacharias et al. 2010) and 2MASS catalogs. Open clusters are valuable targets for probing the Galactic disk and calibrating stellar parameters, and are interesting objects in their own right. Known members of open clusters will be given a high priority of observation. The majority of the targets will be field stars, selected using an algorithm with a weighted random sampling of optical colors and proper motions. Spectra of field stars will be vital for studying the local dynamical and chemical structures, substructures and gradients, moving groups, young stellar objects and three-dimensional extinction in the disk.

Starting from year two or three of the survey, medium resolution ($R = 5\,000$) spectra will be obtained for those most interesting targets discovered among those already observed at $R = 1\,800$. The $R = 5\,000$ spectra will yield precise radial velocities, alpha and other elemental abundances.

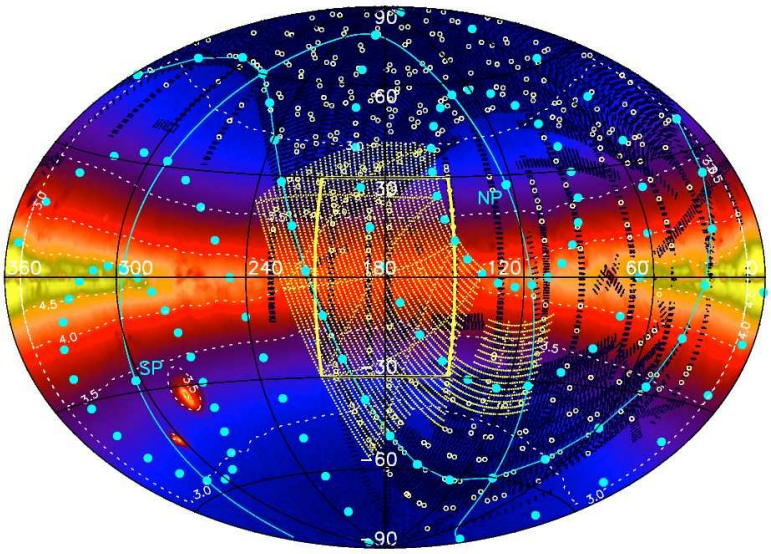

Fig. 6 The DSS-GAC footprint. The Galactic coordinate system in Aitoff projection is used, with the longitude l running from zero at the right to 360 at the left. *Yellow dots*: Survey area of the XSTPS-GAC, the imaging photometric component of the DSS-GAC, covering 3h $\leq$ RA $\leq$ 9h, $-10^\circ \leq$ Dec $\leq +60^\circ$, with an extension to the M 31 and M 33 areas. Each dot represents a field of view of $1.94^\circ \times 1.94^\circ$. Central *yellow box*: Survey area of the GSJTSS-GAC, the spectroscopic component of the DSS-GAC, covering $150^\circ \leq l \leq 210^\circ$ and $-30 \leq b \leq +30^\circ$. Background *pseudo color* image: Stellar density map derived from the 2MASS Point Source Catalog ($10.8 \leq J \leq 15.8$ mag and Ph_Qual = A, B and C for the J, H and Ks bands). *White dashed lines* are stellar number density contours with the logarithmic density per deg^2 labeled. Also overlaid is the equatorial coordinate system, with filled cyan dots delineating constant Dec of -90, -60, -30, 0, +30, +60 and +90 degree, at one hour step in RA. The north and south poles (NP and SP) are marked. The equator and the constant RA lines of 0 and 12 hr are drawn with solid lines. *Black shaded area*: SDSS imaging sky coverage. *White circles*: SDSS SEGUE-I and II spectroscopic plates. (From Liu et al. 2012, in preparation).

4.2 The Digital Sky Survey of the Galactic Anti-center (DSS-GAC)

The anti-center survey, named the Guo Shou Jing Telescope Spectroscopic Survey of the Galactic Anti-center (GSJTSS-GAC), is the spectroscopic component of the Digital Sky Survey of the Galactic Anti-center (DSS-GAC; Liu et al. 2012, in preparation; see Fig. 6). As an integral component of LEGUE, GSJTSS-GAC is of particular relevance for studies of the structure, formation and evolution of the Milky Way galaxy given the fact that the disk is the defining component of a disk galaxy in terms of stellar mass, angular momentum and star formation. The Galactic disk has already been known to exhibit rich yet poorly-understood (sub-)structures. Taking advantage of the fact that GSJTSS-GAC is ideally matched to the seasonal variation of Xinglong's weather conditions (Yao et al. 2012) and the unique capability of LAMOST (4 000 fibers), the survey aims to deliver classifications, radial velocities and stellar parameters ($T_{\rm eff}$, log g, [Fe/H], [α/Fe] and [C/Fe]) for a statistically complete sample of about 4 million stars down to a limiting magnitude of $r = 18.5$, distributed in a contiguous area of 3438 deg^2 ($-30^\circ \leq b \leq +30^\circ, 150^\circ \leq l \leq 210^\circ$) and sampling a significant volume of the Galactic thin/thick disks and of the halo.

4.2.1 The Xuyi Schmidt Telescope Photometric Survey of the Galactic Anti-center (XSTPS-GAC)

There are no deep, public digital imaging surveys in the optical bands that fully cover the GSJTSS-GAC footprint. To provide an input catalog for the GSJTSS-GAC, a Xuyi Schmidt Telescope Photometric Survey of the Galactic Anti-center (XSTPS-GAC, Yuan et al. 2012a, in preparation; Zhang et al. 2012, in preparation), the photometric imaging component of DSS-GAC, has been carried out with the Xuyi 1.04/1.20m Schmidt Telescope in the SDSS g-, r- and i-bands.

XSTPS-GAC covers sky area between 3h $\leq$ RA $\leq$ 9h, $-10^\circ \leq$ Dec $\leq +60^\circ$, with an extension to the M 31 and M 33 areas, totaling approximately 7 000 deg^2. XSTPS-GAC has yielded high quality photometry (2–3 percent) in the SDSS g-, r- and i-bands and astrometry (0.1 arcsec) for about 100 million stars down to a 10σ limiting magnitude about 19. Complementary information from other catalogs, such as Galex (Morrissey et al. 2007), PPMXL (Roeser et al. 2010), UCAC3.0, SDSS, IPHAS (Drew et al. 2005), 2MASS and WISE (Wright et al. 2010), are currently being added to the source catalogs. The catalogs generated by XSTPS-GAC have been used for the LAMOST commissioning observations as well as for the pilot survey of the GSJTSS-GAC. The data will also be an invaluable resource in reducing and follow-up analysis of the LAMOST data. In addition, taking advantage of its sky coverage, accurate photometry and survey depth, the data will be an asset to study and constrain the disk structure (e.g., scale heights and lengths of the thin and thick disks; disk flare, warp and truncation) and substructures (e.g., the Monoceros ring) in the anti-center direction.

4.2.2 Target selection of DSS-GAC

To maximize the discovery space, the basic approach of target selection of DSS-GAC is to uniformly select stars in the $(g-r)$ versus r and $(r-i)$ versus r color-magnitude space (Yuan et al. 2012b, in preparation). The approach has the advantages that: 1) It is based on a simple and well defined selection function, and facilitates recovering the underlying stellar populations being sampled; 2) Stars of all colors (spectral types) and magnitudes (distances) down to a pre-defined limiting magnitude are selected as much and as evenly as possible; 3) Rare stars/objects of extreme colors are preferentially selected and observed.

Based on the actual measured performance of LAMOST, science goals and data quality requirements of DSS-GAC, the bright and faint ends of the limiting magnitudes of DSS-GAC targets have been set at 14.0 and 18.5 in the r-band, respectively. To minimize cross-talks between the adjacent fibers and ensure the spectral signal-to-noise (S/N) ratios are as uniform as possible, the targets are grouped into bright, medium and faint plates. For a given patch of sky out of the Galactic plane ($|b| \geq 3.5^\circ$), the sky is sampled by 1 000 stars per deg^2 by defining two bright, two medium and one faint plate. Within the Galactic plane ($|b| \leq 3.5^\circ$), the sampling rate is doubled. The central bright star and targets of each plate are assigned and checked in advance. In overlapping areas of adjacent fields, repeated observations will be carried out for time-domain spectroscopy. Special targets of small numbers, such as emission line objects from the IPHAS (Witham et al. 2008) and young stellar objects, are also included *ad hoc* in the DSS-GAC.

To investigate targets to be sampled by the DSS-GAC project, simulated target catalogs in a stripe along $l = 180^\circ$ ($-30^\circ \leq b \leq +30^\circ, 179.5^\circ \leq l \leq 180.5^\circ$) have been generated using the Besancon model (Robin et al. 2003) of the Milky Way (Yuan et al. 2012b, in preparation). They find that the survey completeness strongly depends on stellar types, as expected. Most common G dwarfs are sampled to 8 percent. However, stars with very blue or red colors, such as A dwarfs, M dwarfs, K giants and M giants, are sampled to 40 percent or more. In total, about 16 percent of stars in this stripe with $14.0 \leq r \leq 18.5$ are selected. DSS-GAC selects targets from M dwarfs to M giants, permitting the volumes to be probed over a wide range of distances. At $r = 18.5$, M0V, G0V, A0V, K0III and M0III stars can reach about 0.6, 7.7, 25, 40 and 110 kpc, respectively, assuming zero reddening.

4.2.3 Science goals

DSS-GAC aims to deliver classifications, radial velocities and stellar parameters ($T_{\rm eff}$, log g, [Fe/H], [α/Fe] and [C/Fe]) for a statistically complete sample of about 4 million stars down to a limiting magnitude of $r = 18.5$, distributed in a contiguous area of 3438 deg^2 ($-30^\circ \leq b \leq +30^\circ, 150^\circ \leq l \leq 210^\circ$) and sampling a significant volume of the Galactic thin/thick disks and halo. The forthcoming next generation astrometric satellite Gaia (Perryman et al. 2001; Katz et al. 2004) will yield proper motions and distances for one billion Galactic stars to $V \sim 20$, radial velocities of 100–150 million stars to $V \sim$ 17–18, and stellar atmospheric parameters for $\sim$ 5 million stars to $V \sim$ 14-15. Together with measurements of distances and proper motions from Gaia, DSS-GAC will yield a unique dataset with the following goals (Liu et al. 2012, in preparation):

- Study and characterize the stellar populations, chemical composition, kinematics and structure of the thin/thick disks and their interface with the halo as a function of Galactic position via distribution functions;
- Identify tidal streams and debris of disrupted dwarfs and clusters;
- Understand how resilient galaxy disks are after gravitational interactions;
- Study temporal and secular evolution of the disks;
- Probe the gravitational potential and dark matter distribution;
- Map the interstellar extinction as a function of distance;
- Search for rare objects (e.g. stars of peculiar chemical composition and with hyper-velocities);
- Study variable stars and binaries with multi-epoch spectroscopy;
- Ultimately advance our understanding of the assemblage of galaxies and the origin of their regularity and diversity.

4.2.4 Pilot survey of DSS-GAC

The LAMOST pilot survey was initiated in October, 2011 and was completed in June, 2012. In total 67 plates, including 27 bright, 27 medium and 13 faint ones, of 25 fields located along a stripe of constant Dec$= 29^\circ$, were planned for DSS-GAC. In the end, 26 bright, 26 medium and 10 faint plates were observed. In total, about 370 000 spectra of 270 000 stars have been recorded, with 80, 70 and 60 percent of the targets observed achieving a spectral S/N ratio per resolution element at 7150 Å higher than 10, 20 and 30, respectively. Out of those, 21.3, 5.6 and 1.5 percent of the targets were observed 2, 3 and 4 times, respectively.

In the extension region of XSTPS-GAC, 11 fields connecting M 31 and M 33 were also planned for the LAMOST pilot survey. The stellar targets of these fields were selected using the same DSS-GAC target selection algorithm. In total, about 150 000 spectra of 86 000 stars have been recorded, with 80, 68 and 57 percent of the targets observed achieving a spectral S/N ratio at 7150 Å higher than 10, 20 and 30, respectively.

Starting from 2012 January 5, a number of very bright plates were also observed on bright nights around the full moon when the sky background was too high for other plates. Within the XSTPS-GAC survey area, the targets of very bright plates were selected from the XSTPS-GAC and 2MASS catalogs, choosing those with $r \leq 14.0$ and $J \geq 9.0$. Outside the XSTPS-GAC survey area, the targets were selected from the PPMXL and 2MASS catalogs. Till 2012 March 14, about 200 000 spectra of 180 000 stars have been obtained within the XSTPS-GAC survey area, with 80 percent of the targets observed achieving a spectral S/N ratio at 7150 Å higher than 30.

4.3 The South Galactic Cap U-band Sky Survey (SCUSS)

The South Galactic Cap U-band Sky Survey (SCUSS; *http://batc.bao.ac.cn/Uband*; Zhou et al. 2012, in preparation; Fan et al. 2012, in preparation; Wu et al. 2012, in preparation) is an international

cooperative project between NAOC and Steward Observatory. Starting from September, 2010 and expected to be complete in December, 2012, it will image an area of about 3700 deg^2 in the south Galactic cap ($Dec \geq -10°, b \leq -30°$) in the SDSS u-band with the 2.3 m Bok telescope. Although SDSS III has provided the photometric catalog in most of the survey area of SCUSS (see Fig. 6), the latter reaches a limiting magnitude about 1.5 mag deeper than the SDSS in the u-band. Till now, over half of the survey regions have been imaged. All the imaging data have been processed with the SCUSS software pipeline and the data are expected to be released at the end of 2013.

Accurate u-band photometry is very important in characterizing stellar parameters. Due to plenty of metal absorption lines in the u-band, the ultraviolet excess of a blue main-sequence (F and G type) star is correlated with its metallicity (e.g., Wallerstein 1962; Sandage 1969; Carney 1979; Ivezić et al. 2008). The u-band also provides a discriminating power in separating blue horizontal branch stars from blue stragglers and main-sequence A stars (e.g., Deason et al. 2011). Given that the SCUSS achieves 1.5 magnitudes deeper than SDSS in the u-band, the survey is expected to be very helpful for Galactic studies, such as measuring the metallicity distribution function of the halo based on photometric calibrated metallicities and distances, and tracing the halo structure and substructures with blue horizontal branch stars (e.g., Deason et al. 2012).

Note that the survey has made a number of supplementary observations within the XSTPS-GAC footprint. Two regions, one of ~ 400 deg^2 ($65° \leq$ RA $\leq 135°, 0° \leq$ Dec $\leq 5°$) and another of ~ 300 deg^2 around the Galactic anti-center, have been observed. More areas between the Galactic anti-center and SCUSS fields are planned to connect them together in the future.

Acknowledgements M.C.S. wishes to thank Liu Chao for helpful discussions, J. Bovy & S. Garbari for providing the data used in Fig. 2, and V. Debattista for providing the model results in Fig. 1. The authors also wish to thank Doug Lin for his efforts in making KIAA a vibrant international research institute. M.C.S. acknowledges financial support from the Peking University One Hundred Talent Fund (985) and the National Natural Science Foundation of China (Grant Nos. 11173002 and 11010022).

References

Aihara, H., Allende Prieto, C., An, D., et al. 2011, ApJS, 193, 29
Antoja, T., Helmi, A., Bienayme, O., et al. 2012, arXiv:1205.0546
Aoki, W., Arimoto, N., Sadakane, K., et al. 2009, A&A, 502, 569
Balser, D. S., Rood, R. T., Bania, T. M., & Anderson, L. D. 2011, ApJ, 738, 27
Barden, S. C., Jones, D. J., Barnes, S. I., et al. 2010, in Society of Photo-Optical Instrumentation Engineers (SPIE) Conference Series, 7735, 773509
Battaglia, G., Tolstoy, E., Helmi, A., et al. 2006, A&A, 459, 423
Belokurov, V., Zucker, D. B., Evans, N. W., et al. 2006, ApJ, 647, L111
Belokurov, V., Zucker, D. B., Evans, N. W., et al. 2007, ApJ, 654, 897
Belokurov, V., Walker, M. G., Evans, N. W., et al. 2008, ApJ, 686, L83
Bensby, T., Alves-Brito, A., Oey, M. S., Yong, D., & Meléndez, J. 2011, ApJ, 735, L46
Binney, J. 2010, MNRAS, 401, 2318
Binney, J., & Merrifield, M. 1998, Galactic Astronomy
Boeche, C., Siebert, A., Williams, M., et al. 2011, AJ, 142, 193
Bond, N. A., Ivezić, Ž., Sesar, B., et al. 2010, ApJ, 716, 1
Bovy, J. 2010, ApJ, 725, 1676
Bovy, J., Rix, H.-W., Liu, C., et al. 2012a, ApJ, 753, 148
Bovy, J., Rix, H.-W., & Hogg, D. W. 2012b, ApJ, 751, 131
Bovy, J., Rix, H.-W., Hogg, D. W., et al. 2012c, arXiv:1202.2819
Bovy, J., & Tremaine, S. 2012, arXiv:1205.4033

Brook, C. B., Kawata, D., Gibson, B. K., & Freeman, K. C. 2004, ApJ, 612, 894
Brown, T. M., Tumlinson, J., Geha, M., et al. 2012, ApJ, 753, L21
Bullock, J. S., & Johnston, K. V. 2005, ApJ, 635, 931
Carlin, J. L., Lépine, S., Newberg, H. J., et al. 2012, RAA (Research in Astronomy and Astrophysics), 12, 755
Carney, B. W. 1979, ApJ, 233, 211
Carollo, D., Beers, T. C., Chiba, M., et al. 2010, ApJ, 712, 692
Carrera, R., Aparicio, A., Martínez-Delgado, D., & Alonso-García, J. 2002, AJ, 123, 3199
Casetti-Dinescu, D. I., Girard, T. M., Korchagin, V. I., & van Altena, W. F. 2011, ApJ, 728, 7
Chen, L., Hou, J.-L., Yu, J.-C., et al. 2012, RAA (Research in Astronomy and Astrophysics), 12, 805
Cheng, J. Y., Rockosi, C. M., Morrison, H. L., et al. 2012, ApJ, 752, 51
Coleman, M. G., de Jong, J. T. A., Martin, N. F., et al. 2007, ApJ, 668, L43
Cui, X., Su, D., Li, G., et al. 2004, in Society of Photo-Optical Instrumentation Engineers (SPIE) Conference Series, 5489, ed. J. M. Oschmann, Jr., 974
Cui, X., Su, D.-Q., Wang, Y.-N., et al. 2010, in Society of Photo-Optical Instrumentation Engineers (SPIE) Conference Series, 7733, Ground-based and Airborne Telescopes III, ed. L. M. Stepp, R. Gilmozzi, & H. J. Hall, 773309-1-8
de Jong, J. T. A., Yanny, B., Rix, H.-W., et al. 2010, ApJ, 714, 663
De Simone, R., Wu, X., & Tremaine, S. 2004, MNRAS, 350, 627
Deason, A. J., Belokurov, V., & Evans, N. W. 2011, MNRAS, 416, 2903
Deason, A. J., Belokurov, V., Evans, N. W., et al. 2012, arXiv:1205.6203
Dehnen, W. 1998, AJ, 115, 2384
Dehnen, W. 2000, AJ, 119, 800
Dehnen, W., & Binney, J. J. 1998a, MNRAS, 298, 387
Dehnen, W., & Binney, J. 1998b, MNRAS, 294, 429
Deng, L.-C., Newberg, H. J., Liu, C., et al. 2012, RAA (Research in Astronomy and Astrophysics), 12, 735
Dierickx, M., Klement, R., Rix, H.-W., & Liu, C. 2010, ApJ, 725, L186
Drew, J. E., Greimel, R., Irwin, M. J., et al. 2005, MNRAS, 362, 753
Efstathiou, G. 2000, MNRAS, 317, 697
Famaey, B., Jorissen, A., Luri, X., et al. 2005, A&A, 430, 165
Frebel, A., Kirby, E. N., & Simon, J. D. 2010a, Nature, 464, 72
Frebel, A., Simon, J. D., Geha, M., & Willman, B. 2010b, ApJ, 708, 560
Fux, R. 2001, A&A, 373, 511
Garbari, S., Read, J. I., & Lake, G. 2011, MNRAS, 416, 2318
Garbari, S., Liu, C., Read, J. I., & Lake, G. 2012, arXiv:1206.0015
Gilmore, G., & Reid, N. 1983, MNRAS, 202, 1025
Giuffrida, G., Sbordone, L., Zaggia, S., et al. 2010, A&A, 513, A62
Gnedin, N. Y. 2000, ApJ, 542, 535
Gómez, F. A., Minchev, I., Villalobos, Á., O'Shea, B. W., & Williams, M. E. K. 2012a, MNRAS, 419, 2163
Gómez, F. A., Minchev, I., O'Shea, B. W., et al. 2012b, MNRAS, 423, 3727
Helmi, A., Navarro, J. F., Nordström, B., et al. 2006a, MNRAS, 365, 1309
Helmi, A., Irwin, M. J., Tolstoy, E., et al. 2006b, ApJ, 651, L121
Holmberg, J., Nordström, B., & Andersen, J. 2009, A&A, 501, 941
Hurley-Keller, D., Mateo, M., & Nemec, J. 1998, AJ, 115, 1840
Irwin, M. J., Belokurov, V., Evans, N. W., et al. 2007, ApJ, 656, L13
Ishigaki, M. N., Chiba, M., & Aoki, W. 2012, ApJ, 753, 64
Ivezić, Ž., Sesar, B., Jurić, M., et al. 2008, ApJ, 684, 287
Jurić, M., Ivezić, Ž., Brooks, A., et al. 2008, ApJ, 673, 864
Kapteyn, J. C. 1905, British Assoc. Adv. Sci. Rep., Section A, 257-65, 264

Katz, D., Munari, U., Cropper, M., et al. 2004, MNRAS, 354, 1223
Kirby, E. N., Simon, J. D., Geha, M., Guhathakurta, P., & Frebel, A. 2008, ApJ, 685, L43
Kirby, E. N., Lanfranchi, G. A., Simon, J. D., Cohen, J. G., & Guhathakurta, P. 2011, ApJ, 727, 78
Klypin, A., Kravtsov, A. V., Valenzuela, O., & Prada, F. 1999, ApJ, 522, 82
Koch, A., McWilliam, A., Grebel, E. K., Zucker, D. B., & Belokurov, V. 2008, ApJ, 688, L13
Kordopatis, G., Recio-Blanco, A., de Laverny, P., et al. 2011, A&A, 535, A107
Kuijken, K., & Gilmore, G. 1989a, MNRAS, 239, 571
Kuijken, K., & Gilmore, G. 1989b, MNRAS, 239, 605
Kuijken, K., & Gilmore, G. 1989c, MNRAS, 239, 651
Kuijken, K., & Gilmore, G. 1991, ApJ, 367, L9
Larson, R. B. 1974, MNRAS, 169, 229
Lee, Y. S., Beers, T. C., Allende Prieto, C., et al. 2011a, AJ, 141, 90
Lee, Y. S., Beers, T. C., An, D., et al. 2011b, ApJ, 738, 187
Letarte, B., Hill, V., Jablonka, P., et al. 2006, A&A, 453, 547
Liu, C., & van de Ven, G. 2012, arXiv:1201.1635
Liu, C., Xue, X., Fang, M., et al. 2012, ApJ, 753, L24
Loebman, S. R., Roškar, R., Debattista, V. P., et al. 2011, ApJ, 737, 8
Mateo, M. L. 1998, ARA&A, 36, 435
Matteucci, F., & Recchi, S. 2001, ApJ, 558, 351
Minchev, I., & Famaey, B. 2010, ApJ, 722, 112
Minchev, I., Quillen, A. C., Williams, M., et al. 2009, MNRAS, 396, L56
Monelli, M., Pulone, L., Corsi, C. E., et al. 2003, AJ, 126, 218
Moore, B., Ghigna, S., Governato, F., et al. 1999, ApJ, 524, L19
Morrissey, P., Conrow, T., Barlow, T. A., et al. 2007, ApJS, 173, 682
Okamoto, S., Arimoto, N., Yamada, Y., & Onodera, M. 2008, A&A, 487, 103
Okamoto, S., Arimoto, N., Yamada, Y., & Onodera, M. 2012, ApJ, 744, 96
Pancino, E., & Gaia-ESO Survey consortium 2012, in Calibration and Standardization of Large Surveys and Missions in Astronomy and Astrophysics, arXiv:1206.6291
Perryman, M. A. C., de Boer, K. S., Gilmore, G., et al. 2001, A&A, 369, 339
Peter, A. H. G. 2011, Phys. Rev. D, 83, 125029
Quillen, A. C., Dougherty, J., Bagley, M. B., Minchev, I., & Comparetta, J. 2011, MNRAS, 417, 762
Quillen, A. C., & Minchev, I. 2005, AJ, 130, 576
Robin, A. C., Reylé, C., Derrière, S., & Picaud, S. 2003, A&A, 409, 523
Roeser, S., Demleitner, M., & Schilbach, E. 2010, AJ, 139, 2440
Roškar, R., Debattista, V. P., Stinson, G. S., et al. 2008, ApJ, 675, L65
Ruchti, G. R., Fulbright, J. P., Wyse, R. F. G., et al. 2011, ApJ, 737, 9
Sadakane, K., Arimoto, N., Ikuta, C., et al. 2004, PASJ, 56, 1041
Sales, L. V., Helmi, A., Abadi, M. G., et al. 2009, MNRAS, 400, L61
Sandage, A. 1969, ApJ, 158, 1115
Sanders, J. 2012, arXiv:1205.5397
Schönrich, R. 2012, MNRAS, arXiv:1207.3079
Schönrich, R., & Binney, J. 2009a, MNRAS, 396, 203
Schönrich, R., & Binney, J. 2009b, MNRAS, 399, 1145
Schönrich, R., & Binney, J. 2012, MNRAS, 419, 1546
Schönrich, R., Binney, J., & Asplund, M. 2012, MNRAS, 420, 1281
Seabroke, G. M., & Gilmore, G. 2007, MNRAS, 380, 1348
Sellwood, J. A., & Binney, J. J. 2002, MNRAS, 336, 785
Shetrone, M. D., Côté, P., & Sargent, W. L. W. 2001, ApJ, 548, 592

Shetrone, M., Venn, K. A., Tolstoy, E., et al. 2003, AJ, 125, 684
Siebert, A., Williams, M. E. K., Siviero, A., et al. 2011a, AJ, 141, 187
Siebert, A., Famaey, B., Minchev, I., et al. 2011b, MNRAS, 412, 2026
Smecker-Hane, T. A., Stetson, P. B., Hesser, J. E., & Lehnert, M. D. 1994, AJ, 108, 507
Smith, M. C., Evans, N. W., Belokurov, V., et al. 2009, MNRAS, 399, 1223
Smith, M. C., Whiteoak, S. H., & Evans, N. W. 2012, ApJ, 746, 181
Somerville, R. S. 2002, ApJ, 572, L23
Spagna, A., Lattanzi, M. G., Re Fiorentin, P., & Smart, R. L. 2010, A&A, 510, L4
Su, D. Q., Cui, X., Wang, Y., & Yao, Z. 1998, in Society of Photo-Optical Instrumentation Engineers (SPIE) Conference Series, 3352, ed. L. M. Stepp, 76
Susa, H., & Umemura, M. 2004, ApJ, 600, 1
Tafelmeyer, M., Jablonka, P., Hill, V., et al. 2010, A&A, 524, A58
Tinsley, B. M. 1979, ApJ, 229, 1046
Tolstoy, E., Venn, K. A., Shetrone, M., et al. 2003, AJ, 125, 707
Tolstoy, E., Hill, V., & Tosi, M. 2009, ARA&A, 47, 371
van den Bergh, S. 1999, A&A Rev., 9, 273
van der Kruit, P. C., & Freeman, K. C. 2011, ARA&A, 49, 301
Venn, K. A., Irwin, M., Shetrone, M. D., et al. 2004, AJ, 128, 1177
Wallerstein, G. 1962, ApJS, 6, 407
Walsh, S. M., Willman, B., Sand, D., et al. 2008, ApJ, 688, 245
Wang, S.-G., Su, D.-Q., Chu, Y.-Q., Cui, X., & Wang, Y.-N. 1996, Appl. Opt., 35, 5155
Widrow, L. M., Gardner, S., Yanny, B., Dodelson, S., & Chen, H.-Y. 2012, ApJ, 750, L41
Willman, B., Dalcanton, J. J., Martinez-Delgado, D., et al. 2005, ApJ, 626, L85
Wilson, M. L., Helmi, A., Morrison, H. L., et al. 2011, MNRAS, 413, 2235
Witham, A. R., Knigge, C., Drew, J. E., et al. 2008, MNRAS, 384, 1277
Wright, E. L., Eisenhardt, P. R. M., Mainzer, A. K., et al. 2010, AJ, 140, 1868
Xing, X., Zhai, C., Du, H., et al. 1998, in Society of Photo-Optical Instrumentation Engineers (SPIE) Conference Series, 3352, ed. L. M. Stepp, 839
Yang, F., Carlin, J. L., Liu, C., et al. 2012, RAA (Research in Astronomy and Astrophysics), 12, 781
Yanny, B., Rockosi, C., Newberg, H. J., et al. 2009, AJ, 137, 4377
Yao, S., Liu, C., Zhang, H.-T., et al. 2012, RAA (Research in Astronomy and Astrophysics), 12, 772
York, D. G., Adelman, J., Anderson, J. E., Jr., et al. 2000, AJ, 120, 1579
Yu, J., Sellwood, J. A., Pryor, C., Chen, L., & Hou, J. 2012, arXiv:1205.7001
Zacharias, N., Finch, C., Girard, T., et al. 2010, AJ, 139, 2184
Zentner, A. R., & Bullock, J. S. 2003, ApJ, 598, 49
Zhang, Y.-Y., Carlin, J. L., Yang, F., et al. 2012, RAA (Research in Astronomy and Astrophysics), 12, 792
Zhao, G., Zhao, Y.-H., Chu, Y.-Q., Jing, Y.-P., & Deng, L.-C. 2012, RAA (Research in Astronomy and Astrophysics), 12, 723
Zhao, Y. 2000, in Society of Photo-Optical Instrumentation Engineers (SPIE) Conference Series, 4010, ed. P. J. Quinn, 290
Zhu, Y., Hu, Z., Zhang, Q., Wang, L., & Wang, J. 2006, in Society of Photo-Optical Instrumentation Engineers (SPIE) Conference Series, 6269, 20
Zucker, D. B., Belokurov, V., Evans, N. W., et al. 2006a, ApJ, 643, L103
Zucker, D. B., Belokurov, V., Evans, N. W., et al. 2006b, ApJ, 650, L41